Theoretical Study of the Equilibrium Structure, Vibrational Spectrum, and Thermochemistry of the Peroxynitrate CF2BrCFBrOONO2

ARTICLE *in* THE JOURNAL OF PHYSICAL CHEMISTRY A · JUNE 2011

Impact Factor: 2.69 · DOI: 10.1021/jp2018617 · Source: PubMed

3 AUTHORS, INCLUDING:

María Badenes
National University of La Plata
20 PUBLICATIONS **122** CITATIONS
SEE PROFILE

Carlos J. Cobos
National Scientific and Technical Research C…
126 PUBLICATIONS **3,053** CITATIONS
SEE PROFILE

THE JOURNAL OF PHYSICAL CHEMISTRY A

ARTICLE

pubs.acs.org/JPCA

Theoretical Study of the Equilibrium Structure, Vibrational Spectrum, and Thermochemistry of the Peroxynitrate $CF_2BrCFBrOONO_2$

María P. Badenes,* Larisa L. B. Bracco, and Carlos J. Cobos

Instituto de Investigaciones Fisicoquímicas Teóricas y Aplicadas (INIFTA), Departamento de Química, Facultad de Ciencias Exactas, Universidad Nacional de La Plata, Casilla de Correo 16, Sucursal 4, (1900) La Plata, Argentina

ABSTRACT: The results of a theoretical study of the molecular structure and conformational mobilities of the peroxynitrate $CF_2BrCFBrOONO_2$ and its radical decomposition product $CF_2BrCFBrOO$ are reported in this paper. The most stable structures were calculated from ab initio G3(MP2)B3 and G4(MP2) methods and from density functional theory at the B3LYP/6-311+G(d) and B3LYP/6-311+G(3df) levels of theory. The equilibrium conformation of $CF_2BrCFBrOONO_2$ indicates that the bromine atoms lie in position *anti* to each other and possess a COON dihedral angle of 114°. A quantum statistical analysis shows that about 40% of the internal rotors can freely rotate at room temperature. Our best values for the standard enthalpies of formation of $CF_2BrCFBrOONO_2$ and $CF_2BrCFBrOO$ at 298 K obtained from isodesmic reactions at the G3(MP2)//B3LYP/6-311+G(3df) level of theory are −144.7 and −127.0 kcal mol^{-1}. From these values and the enthalpy of formation of the NO_2 radical, a $CF_2BrCFBrOO$-NO_2 bond dissociation enthalpy of 26.0 ± 2 kcal mol^{-1} was estimated.

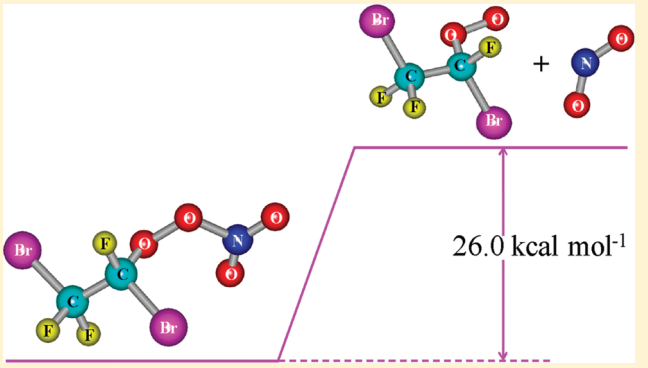

1. INTRODUCTION

As has been reported, peroxynitrates ($ROONO_2$) are thermally unstable intermediates in the atmospheric degradation of hydrocarbons.[1−4] In particular, organic peroxynitrates have been extensively studied due to their importance in atmospheric chemistry.[1−23] The most abundant peroxyacetyl nitrate, $CH_3C(O)OONO_2$ (PAN), is present throughout the global troposphere. Less abundant are halogenated peroxynitrates resulting from the atmospheric degradation of CFC or their replacements.

In a recent work, a new peroxynitrate was reported.[24] This one was obtained as a product in the gas-phase oxidation of CF_2CFBr initiated by the addition of NO_2 to the double bond of an alkene. In such reactions, NO_2 can act as a nitrating and oxidating agent. The main product obtained in the mentioned reaction was $CF_2BrC(O)F$, minor amounts of F_2CO and FBrCO, and small quantities of bromotrifluoroethene epoxide and peroxynitrate $CF_2BrCFBrOONO_2$ were also identified. The rate coefficient for the unimolecular decomposition of this peroxynitrate, $CF_2BrCFBrOONO_2 \rightarrow CF_2BrCFBrOO + NO_2$, was reported at 313.4 K. To our knowledge, no experimental or theoretical data about the structure or bond dissociation energy of $CF_2BrCFBrOONO_2$ have been reported.

In this work, characterization from a theoretical point of view of $CF_2BrCFBrOONO_2$ has been performed. In particular, the torsional potentials connecting the different conformers of both $CF_2BrCFBrOONO_2$ and the $CF_2BrCFBrOO$ radical have been calculated. The equilibrium conformations and harmonic vibrational frequencies of both species are also reported. Furthermore, the enthalpies of formation of the most stable species have been here determined for the first time, and from them the dissociation enthalpy of the $CF_2BrCFBrOO-NO_2$ bond was estimated.

2. COMPUTATIONAL DETAILS

All calculations were performed with the Gaussian 09 program package.[25] The popular hybrid B3LYP density functional, which employs Becke's three-parameter nonlocal exchange functional[26,27] together with the nonlocal correlation functional of Lee, Yang, and Parr,[28] was used to calculate the potentials for the internal rotations of $CF_2BrCFBrOONO_2$ and $CF_2BrCFBrOO$. The 6-311+G(d) split-valence Pople basis set was selected for this case.[29] The optimized geometrical parameters and harmonic vibrational frequencies for the different conformers of $CF_2BrCFBrOONO_2$ and its radical decomposition product were obtained using an analytical gradient and analytical second derivatives methods at the B3LYP/6-311+G(d) and B3LYP/6-311+G(3df) levels of theory. The extended triple split-valence basis set confers remarkable flexibility to represent regions of high electron density among the bonded atoms and far from the nuclei. The unscaled vibrational frequencies were used to evaluate the zero-point energies (ZPE) and the vibrational contribution to the thermal correction at 298.15 K.

Received: February 25, 2011
Revised: May 18, 2011
Published: May 19, 2011

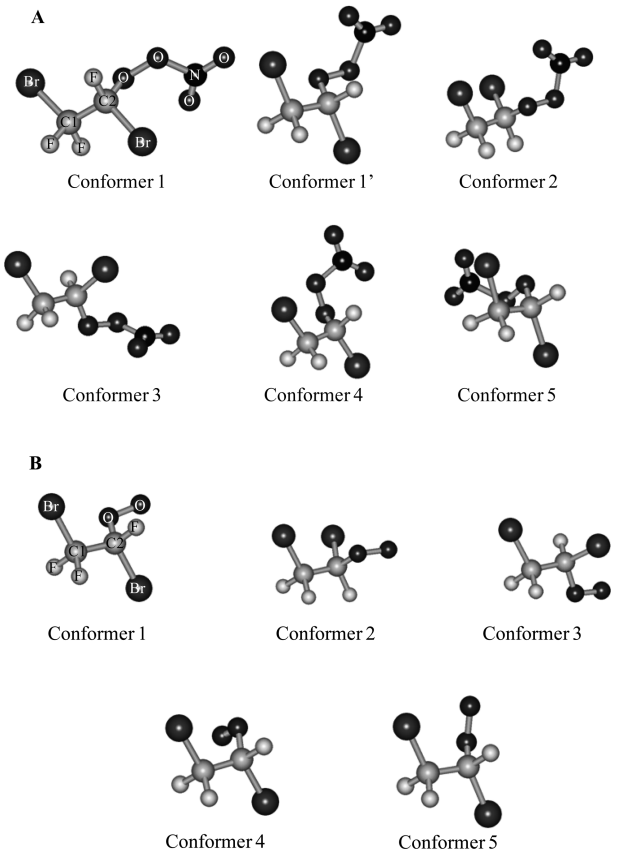

Figure 1. Molecular geometries of the different conformers of (A) $CF_2BrCFBrOONO_2$ and (B) $CF_2BrCFBrOO$ optimized at the B3LYP/6-311+G(3df) level of theory.

More accurate estimates were carried out by using the G3(MP2)B3[30,31] and G4(MP2)[32] model chemistries. In the G3(MP2)B3 method, the optimized molecular structure and harmonic vibrational frequencies (scaled by a factor 0.96) are calculated at the B3LYP/6-31G(d) level. On the basis of the optimized structure, the energy at 0 K is obtained from a set of single-point energy evaluations at the levels MP2/6-31G(d), QCISD(T)/6-31G(d), and MP2(full)/GTMP2Large. Spin−orbit (SO), higher-level (HLC), and zero-point vibrational energy (ZPE) corrections used to calculate the total electronic energy at 0 K were performed a posteriori.[30,31]

The G4(MP2) model is a modification of the G4 method in which second-order perturbation theory is used instead of fourth-order perturbation theory.[32] It uses B3LYP/6-31G(2df,p) optimized geometries and harmonic vibrational frequencies (scaled by 0.9854) followed by a series of single-point energy calculations at higher levels of theory. The first single-point energy calculation is performed at the triples-augmented coupled cluster level of theory, CCSD(T), with the 6-31G(d) basis set. This energy is then modified by a series of energy corrections to obtain a total energy E_0

$$E_0[\mathrm{G4(MP2)}] = \mathrm{CCSD(T)/6\text{-}31G(d)} + \Delta E_{\mathrm{MP2}} + \Delta E_{\mathrm{HF}} + \Delta E(\mathrm{SO}) + E(\mathrm{HLC}) + E(\mathrm{ZPE}) \quad \text{(I)}$$

where the correction at the second-order Moller−Pleset level ΔE_{MP2} is given by the difference between E(MP2)/G3MP2LargeXP and E(MP2)/6-31G(d), and $\Delta E_{\mathrm{HF}} = E(\mathrm{HF/limit}) - E(\mathrm{HF/G3MP2LargeXP})$. The other corrections to E_0 are similar to those in G4 theory. It is found that this method gives significantly improved results compared to G3(MP2) and full G3 theories at less computational cost. The average absolute deviation of the G4(MP2) estimations from well-known experimental heats of formation values is close to the typical chemical accuracy of about 1 kcal mol^{-1}.[32]

Finally, to investigate the influence of the uncertainties in both molecular structures and vibrational frequencies on computed G3(MP2) and G4(MP2) energies, the modified methods, G3(MP2)//B3LYP/6-311+G(3df) and G4(MP2)//B3LYP/6-311+G(3df), were employed. For this, single-point energy calculations, by instance as detailed in eq I, were carried out on optimized B3LYP/6-311+G(3df) structures.

3. RESULTS AND DISCUSSION

3.1. Torsional Barriers for $CF_2BrCFBrOONO_2$. $CF_2BrCFBrOONO_2$ exhibits the five rotational conformers shown in Figure 1A. To study the different conformations of $CF_2BrCFBrOONO_2$, we have performed a potential energy scan of the four possible internal rotations, that is, around the C−C, C−O, O−O, and O−N bonds. To compute the electronic barriers, the corresponding torsional angle was varied in steps of 20° while allowing the optimization of the remaining geometrical parameters at each step. The local and global minima corresponding to different conformers and the maxima corresponding to transition states were fully optimized. To derive the potential function $V(\Phi)$ for the internal rotation, the truncated Fourier expansion (II) was used for the potential computed at the B3LYP/6-311+G(d) level of theory. That is

$$V(\Phi) = a_0 + \sum a_i \cos(i\Phi) + \sum b_i \sin(i\Phi) \quad \text{(II)}$$

where $i = 1-4$. The values of the coefficients a_i and b_i are listed in Table 1. The calculated electronic potentials for all internal rotations are shown in Figures 2, 3, and 4. As can be seen in these figures, excellent fits with standard deviations S_y smaller than about 0.05 kcal mol^{-1} and squared correlation coefficients r^2 better than 0.997 were obtained.

Figure 2a shows the calculated rotational barriers around the C−C bond. This rotation leads to three different conformers. These conformations are different from each other in the BrCCBr dihedral angle. In the most stable conformer, this angle is close to 180°; that is, in the most stable conformation the bromine atoms are as far away from each other as possible (conformer 1). The other conformers, with dihedral angles of about 300° and 60°, are 1.1 and 1.2 kcal mol^{-1} less stable as calculated at the B3LYP/6-311+G(3df) level (conformers 2 and 3). These conformers are separated by two barriers of 6.1 and 8.4 kcal mol^{-1} (imaginary vibrational frequencies, ν, of 44i, 45i, and 48i cm^{-1}, respectively) at the same level. The last barrier corresponds to the structure with a dihedral angle of almost 0°, in which both bromine atoms are in close proximity. Figure 2b shows the calculated symmetric potential energy curves corresponding to rotation around the O−N bond. The two minima are equivalent, corresponding to conformer 1. This rotation does not lead to different conformers because the rotating group, NO_2, possesses an axis of symmetry. For this case, B3LYP/6-311+G(3df) rotational barriers of 9.7 kcal mol^{-1} (ν = 86i cm^{-1}) were computed. The potential energy curve for rotation around the C−O bond is presented in Figure 3. In this case, three

Table 1. Coefficients of the Fourier Expansion for Torsional Potentials of $CF_2BrCFBrOONO_2$ and $CF_2BrCFBrOO$ Calculated at the B3LYP/6-311+G(d) Level of Theory

coefficient	rotations					
(kcal mol^{-1})	$CF_2Br-CFBrOONO_2$	$CF_2BrCFBrOO-NO_2$	$CF_2BrCFBr-OONO_2$	$CF_2BrCFBrO-ONO_2$	$CF_2Br-CFBrOO$	$CF_2BrCFBr-OO$
a_0	3.705	4.481	3.409	6.273	3.775	1.968
a_1	1.170	−0.134	1.899	7.185	1.134	1.424
a_2	0.430	−4.621	0.216	4.331	0.450	0.329
a_3	2.958	0.148	1.388	−0.291	3.100	0.609
a_4	-	-	−0.402	−0.119	-	−0.224
b_1	6.173×10^{-3}	-6.920×10^{-2}	−0.991	0.829	-2.762×10^{-2}	0.192
b_2	4.452×10^{-2}	0.155	−0.722	0.767	5.068×10^{-2}	0.508
b_3	−0.188	-7.086×10^{-2}	-1.853×10^{-3}	−0.144	-8.131×10^{-2}	8.529×10^{-2}
b_4	-	-	-6.605×10^{-2}	-1.328×10^{-2}	-	7.362×10^{-2}

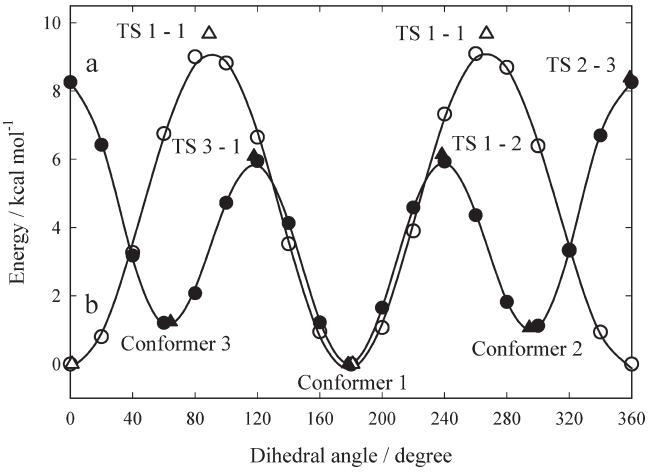

Figure 2. Potential energy barriers for internal rotation around (a) C−C and (b) O−N in $CF_2BrCFBrOONO_2$. Circles: calculated at the B3LYP/6-311+G(d) level. Triangles: calculated at the B3LYP/6-311+G(3df) level. Line: Fourier analysis with the coefficient of Table 1.

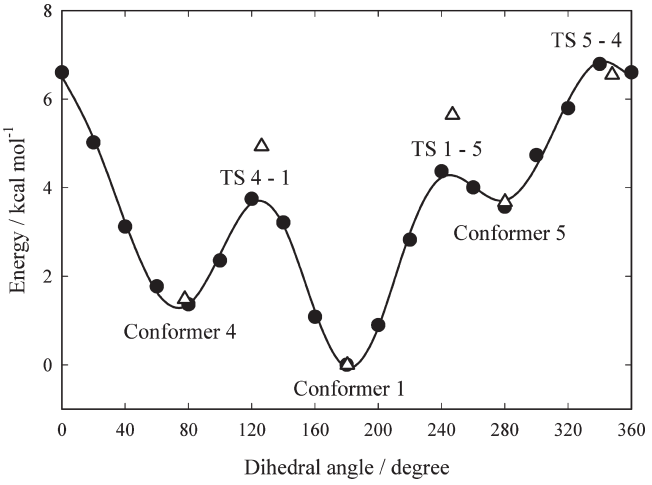

Figure 3. Potential energy barriers for internal rotation around C−O in $CF_2BrCFBrOONO_2$. Circles: calculated at the B3LYP/6-311+G(d) level. Triangles: calculated at the B3LYP/6-311+G(3df) level. Line: Fourier analysis with the coefficient of Table 1.

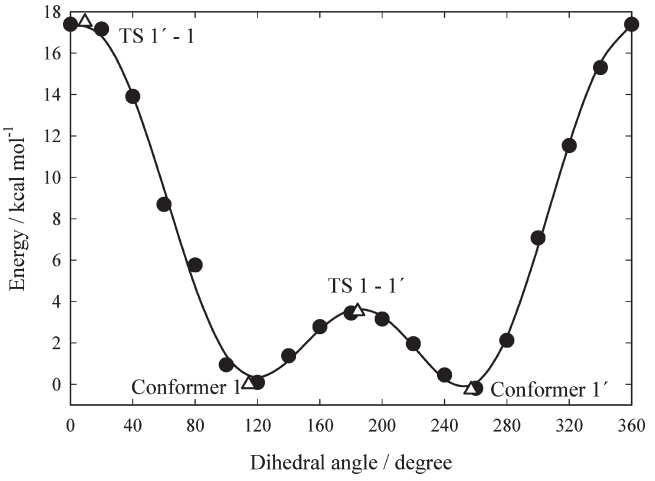

Figure 4. Potential energy barriers for internal rotation around O−O in $CF_2BrCFBrOONO_2$. Circles: calculated at the B3LYP/6-311+G(d) level. Triangles: calculated at the B3LYP/6-311+G(3df) level. Line: Fourier analysis with the coefficient of Table 1.

minima and three maxima are observed. As Figure 1A shows, the global minimum corresponds to a structure with the C2−Br bond oriented toward the plane formed by the $OONO_2$ group and the other C−Br bond *anti* relative to the former (conformer 1). The rotamers 4 and 5 are 1.5 and 3.7 kcal mol^{-1} less stable than the conformer 1 at the B3LYP/6-311+G(3df) level. At the same level of theory, barriers between minima 1 and 5 of 5.7 kcal mol^{-1}, between 5 and 4 of 6.7 kcal mol^{-1}, and between 4 and 1 of 4.9 kcal mol^{-1} were estimated. The imaginary vibrational frequencies for these transition states are 37i, 52i, and 43i cm^{-1}, respectively. Therefore, each of the C−O and C−C rotations causes three conformational isomers, whereas rotation about the N−O bond does not generate new conformers. Finally, as Figure 4 shows, the rotation around the O−O bond leads to two minima and two maxima. By contrast with the previous cases, the minima do not correspond to different conformational isomers but to optical isomers (1 and 1′). They are separated by a high electronic barrier of 17.5 kcal mol^{-1} (ν = 182i cm^{-1}) at a dihedral angle of about 9° and a lower barrier of 3.5 kcal mol^{-1} (ν = 42i cm^{-1}) at about 180°.

3.2. Torsional Barriers for $CF_2BrCFBrOO$. In a similar way, we studied the internal rotations in the $CF_2BrCFBrOO$ radical.

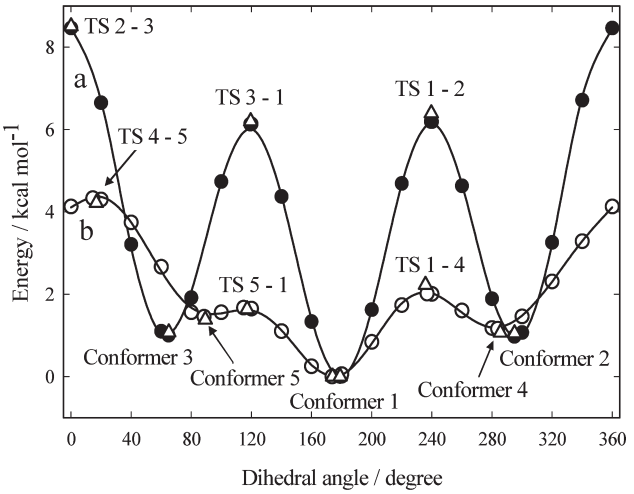

Figure 5. Potential energy barriers for internal rotation around (a) C−C and (b) C−O in $CF_2BrCFBrOO$. Circles: calculated at the B3LYP/6-311+G(d) level. Triangles: calculated at the B3LYP/6-311+G(3df) level. Line: Fourier analysis with the coefficient of Table 1.

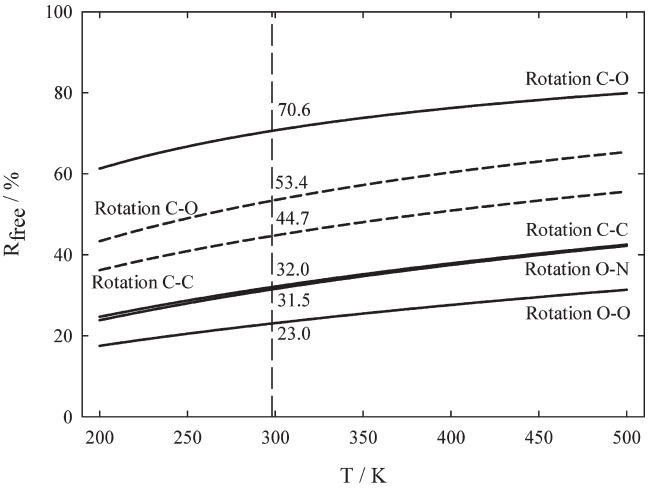

Figure 6. Calculated percentages of molecules with free internal rotations for $CF_2BrCFBrOONO_2$ (solid lines) and $CF_2BrCFBrOO$ (dash lines). The vertical dashed line indicates the 298 K temperature.

This one exhibits two rotations, around the C−C and C−O bonds. All rotamers are displayed in Figure 1B. As before, the calculated rotational potentials have been fitted by use of the truncated Fourier series. The values of the coefficients are listed in Table 1. The $CF_2BrCFBrOO$ potentials exhibit characteristics quite similar to the potentials in $CF_2BrCFBrOONO_2$. For instance, as curve a of Figure 5a shows, rotation about the C−C bond in $CF_2BrCFBrOO$ presents three minima which correspond to conformers 1, 2, and 3. These conformers differ in 1.1 kcal mol^{-1} at the B3LYP/6-311+G(3df) level, and the potential fits almost perfectly the corresponding potential of $CF_2BrCFBrOONO_2$. Moreover, its potential presents barriers of 6.2, 6.4, and 8.5 kcal mol^{-1} (ν = 49i, 51i, and 55i cm^{-1}, respectively), that is, very close to the same barriers of $CF_2BrCFBrOONO_2$. However, in the case of the rotation around the C−O bond, the calculated barriers are about 50% smaller than those estimated for $CF_2BrCFBrOONO_2$. This can be attributed to the C−O bond length in the radical which is about 3.5% longer than the same bond in the peroxynitrate. The rotating group is also smaller in the radical than the peroxynitrate. As Figure 5b shows, the mentioned potential exhibits three barriers of 1.6, 2.2, and 4.2 kcal mol^{-1} (ν = 68i, 86i, and 74i cm^{-1}). Furthermore, this potential presents three minima corresponding to conformers 1, 4, and 5. The computed energies for the last conformers are 1.1 and 1.4 kcal mol^{-1} higher than conformer 1. In conclusion, we found five rotamers for the $CF_2BrCFBrOO$ radical, of which conformer 1 is the most stable (Figure 1).

3.3. Free Internal Rotational Populations for $CF_2BrCFBrOONO_2$ and $CF_2BrCFBrOO$. Subsequently, the rotations of $CF_2BrCFBrOONO_2$ and $CF_2BrCFBrOO$ were analyzed to determine if they are free, partially, or totally restricted at room temperature. For that, we calculated the population of molecules with free internal rotation about a particular bond using the information derived from computed rotational potentials and harmonic vibrational frequencies. This analysis is completely analogous to what has been performed for APAN and PPN peroxynitrates.[33,34] In this procedure, we derived the percentage of molecules with free internal rotation around a particular bond using[35]

$$R_{free} = 100\{[\exp(RT/V_0) - 1]^{-1.2} Q_{tors}/Q_{free} + 1\}^{-1} \quad \text{(III)}$$

where V_0 is the barrier height and Q_{tors} and Q_{free} are partition functions computed considering internal rotations as totally restricted (torsions) and as completely free, respectively. To evaluate Q_{tors} we use the corresponding torsional frequency, and to calculate Q_{free} it was necessary to estimate the reduced moment of inertia for the given rotation, $I_m = I_A I_B/(I_A + I_B)$.

All properties used were computed with B3LYP/6-311+G(3df) energies. The calculated R_{free} values were represented as a function of temperature in Figure 6. As the figure shows, all the curves have similar characteristics. In both cases, the rotation about the C−O bond presents the smallest barrier and therefore possesses the highest percentage of molecules with free internal rotation (about 70% for $CF_2BrCFBrOONO_2$ and about 53% for $CF_2BrCFBrOO$ at room temperature). In the case of the rotation about the C−C bond, the barrier is very similar for $CF_2BrCFBrOONO_2$ and $CF_2BrCFBrOO$; however, the percentage of molecules with free internal rotation around this particular bond is less in the peroxynitrate. This is due to the large moiety present in the last. On average, about 39% of the moieties of $CF_2BrCFBrOONO_2$ can rotate freely and about 49% in the case of $CF_2BrCFBrOO$, at 298 K.

3.4. Molecular Structures and Harmonic Vibrational Frequencies. The geometrical parameters and harmonic vibrational frequencies for the global minimum structures of $CF_2BrCFBrOONO_2$ and $CF_2BrCFBrOO$ were obtained using the hybrid B3LYP density functional in conjunction with the extended 6-311+G(3df) basis set. At this level of theory, the frequency scaling factor is expected to be close to unity.[36] The calculated structural parameters are presented in Table 2. The most stable conformation of $CF_2BrCFBrOONO_2$ exhibits the bromine atoms in position *anti* to each other and possesses a COON dihedral angle of 114.3°. The peroxynitrates with two sp^2-hybridized groups (RC(O) and NO_2) present dihedral angles close to 90°, whereas peroxynitrates with two sp^3-hybridized groups show dihedral angles of 120°.[33,34,37,38] In the case of $CF_2BrCFBrOONO_2$, the dihedral angle is slightly smaller than

dx.doi.org/10.1021/jp2018617 |J. Phys. Chem. A 2011, 115, 7744–7752

Table 2. Geometrical Parameters of $CF_2BrCFBrOONO_2$ and $CF_2BrCFBrOO$ Calculated at the B3LYP/6-311+G(3df) Level of Theory (Bond Lengths in Angstroms and Angles in Degrees)

parameter	$CF_2BrCFBrOONO_2$	$CF_2BrCFBrOO$
r(C1−Br)	1.959	1.957
r(C2−Br)	1.970	1.953
r(C1−C2)	1.564	1.560
r(C1−F)$_{mean}$	1.334	1.340
r(C2−F)	1.343	1.339
r(C−O)	1.383	1.431
r(O−O)	1.406	1.320
r(N−O)	1.542	-
r(N═O)$_{mean}$	1.180	-
∠(BrC1F)$_{mean}$	108.9	109.1
∠(BrC1C2)	111.5	111.5
∠(C1C2Br)	109.7	111.2
∠(C1C2F)	109.3	109.9
∠(C1C2O)	105.7	105.8
∠(C2OO)	110.6	112.7
∠(OON)	108.6	-
∠(ON=O)	112.4	-
DIH(BrC1C2Br)	178.2	179.0
DIH(C1C2OO)	179.6	173.6
DIH(C2OON)	114.3	-

the last value and the values of other peroxides and peroxynitrates with the mentioned characteristic. For example, CF_3OOCF_3 and CH_3OOCH_3 display dihedral angles of 132.3° and 119°, respectively.[37,39] However, the peroxynitrate CF_3OONO_2 possesses a COON dihedral angle of 105.1°.[38] The calculated dihedral angle for $CF_2BrCFBrOONO_2$ is between the mentioned values.

Peroxynitrate $CF_2BrCFBrOONO_2$ exhibits a rather long O−N bond of 1.542 Å and a short O−O bond of 1.406 Å, which is very close to the values found in related compounds like CF_3OONO_2 (1.523 and 1.414 Å),[38] $FC(O)OONO_2$ (1.514 and 1.420 Å),[40] $CF_3C(O)OONO_2$ (1.526 and 1.408 Å),[41] and $CF_3OC(O)OONO_2$ (1.551 and 1.399 Å).[42] The long O−N distance is an indicator of a weak bond suggesting a primary thermal dissociation pathway for $CF_2BrCFBrOONO_2$ into the $CF_2BrCFBrOO$ and NO_2.

The harmonic vibrational frequencies and infrared intensities computed for the most stable conformers of $CF_2BrCFBrOONO_2$ and $CF_2BrCFBrOO$ are listed in Table 3. In addition, mode assignments, obtained from the animation of the normal modes and by comparison with species with similar groups, are included. However, a great majority of the modes are strongly coupled with each other, and therefore only approximate assignations are given.

The NO_2 symmetric and asymmetric stretching modes are observed at wavenumbers slightly higher than other peroxynitrates.[43−46] However, the C−O and O−O stretching modes appear at about 1000 and 950 cm^{-1} like other halogenated peroxynitrates.[43,44] Also, the C−F and C−Br stretches are observed at an energy similar to the other halogenated species.[47] Finally, the computed frequencies of the $CF_2BrCFBrOO$ radical are close to the same corresponding modes in $CF_2BrCFBrOONO_2$.

Table 3. Harmonic Vibrational Frequencies (in cm^{-1}), Approximated Assignations, and Infrared Intensities (Between Parentheses in km mol^{-1}) for $CF_2BrCFBrOONO_2$ and $CF_2BrCFBrOO$ Calculated at the B3LYP/6-311+G(3df) Level of Theory

assignation	$CF_2BrCFBrOONO_2$	$CF_2BrCFBrOO$
str asym NO_2	1830 (391)	-
str sym NO_2	1357 (256)	-
str C−C	1223 (37)	1238 (31)
str asym CF_2	1170 (138)	1167 (215)
str C2−F	1120 (178)	1129 (100)
str C−O	1064 (248)	929 (85)
out of plane C2	1010 (42)	-
str O−O	962 (52)	1190 (59)
bend NO_2	824 (192)	-
str C1−Br	795 (301)	1020 (63)
str C2−Br	-	780 (266)
bend NOO	754 (39)	-
bend CCO	-	679 (70)
out of plane N	736 (21)	-
bend CF_2	632 (20)	623 (23)
rock NO_2	626 (22)	-
rock CF_2	-	492 (0.5)
str O−N	514 (28)	-
bend FCC	483 (6)	-
deformation CF_2	-	386 (2)
out of plane O1	410 (0.7)	346 (0.1)
bend FCBr	350 (1)	334 (0.1)
bend FCC	339 (0.3)	-
bend FCCF	317 (0.1)	313 (0.03)
wag CF_2	301 (0.1)	300 (0.3)
bend FCOO	-	254 (0.9)
deformation	-	182 (0.5)
out of plane O2	276 (6)	-
bend OONO	242 (0.5)	170 (0.1)
bend FCCBr	189 (0.3)	121 (0.6)
wag CFBr	159 (0.4)	-
wag NO_2	138 (0.1)	-
torsion C−O	114 (0.2)	87 (0.4)
torsion O−N	84 (0.1)	-
torsion C−C	63 (0.1)	52 (0.2)
torsion O−O	50 (0.1)	-

3.5. Thermochemistry. Enthalpies of formation of $CF_2BrCFBrOONO_2$ and $CF_2BrCFBrOO$ were computed from atomization energies and from isodesmic (equal bond) and isogyric reactions. The first approach was used to derive the enthalpies of formation at 0 K, $\Delta H_{f,0}$, by subtracting the computed total atomization energies from the experimental enthalpies of formation of the bromine (28.18 ± 0.01 kcal mol^{-1}),[48] carbon (169.98 ± 0.1 kcal mol^{-1}), fluorine (18.47 ± 0.07 kcal mol^{-1}), nitrogen (112.53 ± 0.02 kcal mol^{-1}), and oxygen atoms (58.99 ± 0.02 kcal mol^{-1}).[49] Estimated thermal contributions and $H^\circ_{298.15} - H^\circ_0$ values for carbon, bromine, fluorine, nitrogen, and oxygen atoms of 0.25, 2.93, 1.05, 1.04, and 1.04 kcal mol^{-1} were employed afterward to transform enthalpies of formation to 298 K, $\Delta H_{f,298}$.[48,49] The resulting thermodynamic values using

dx.doi.org/10.1021/jp2018617 |J. Phys. Chem. A 2011, 115, 7744–7752

Table 4. Calculated Atomization Energies and Enthalpies of Formation for $CF_2BrCFBrOONO_2$ and $CF_2BrCFBrOO$ (in kcal mol^{-1})

	$CF_2BrCFBrOONO_2$			$CF_2BrCFBrOO$		
level of theory	ΣD_0	$\Delta H_{f,0K}$	$\Delta H_{f,298}$	ΣD_0	$\Delta H_{f,0K}$	$\Delta H_{f,298}$
B3LYP/6-311+G(d)	902.4	−102.2	−108.6	664.7	−95.0	−100.0
B3LYP/6-311+G(3df)	931.5	−131.2	−137.9	685.4	−115.7	−120.8
G3(MP2)B3	939.8	−139.6	−145.9	693.0	−123.3	−128.2
G3(MP2)//B3LYP/6-311+G(3df)	938.9	−138.7	−145.4	692.8	−123.1	−128.2
G4(MP2)	936.2	−136.1	−142.5	693.9	−124.3	−129.3
G4(MP2)//B3LYP/6-311+G(3df)	935.6	−135.4	−142.0	693.8	−124.1	−129.2

Table 5. Isodesmic Reactions, Calculated Enthalpy Changes, and Enthalpies of Formation (in kcal mol^{-1}) for $CF_2BrCFBrOONO_2$ and $CF_2BrCFBrOO$

iodesmic reactions

$CF_2BrCFBrOONO_2$

$$HNO_3 + H_2O_2 + CH_3OH + CH_3CH_2Br + CF_3Br \rightarrow CF_2BrCFBrOONO_2 + 2H_2O + 2CH_4 \quad (1)$$

$$HNO_3 + H_2O_2 + CH_3OH + CH_3CF_3 + 2CH_3Br \rightarrow CF_2BrCFBrOONO_2 + 2H_2O + 3CH_4 \quad (2)$$

$$HOONO_2 + CH_3OH + CH_3CH_2Br + CF_3Br \rightarrow CF_2BrCFBrOONO_2 + H_2O + 2CH_4 \quad (3)$$

$$HOONO_2 + CH_3OH + CH_3CF_3 + 2CH_3Br \rightarrow CF_2BrCFBrOONO_2 + H_2O + 3CH_4 \quad (4)$$

$CF_2BrCFBrOO$

$$H_2O_2 + CH_3O + CH_3CH_2Br + CF_3Br \rightarrow CF_2BrCFBrOO + H_2O + 2CH_4 \quad (5)$$

$$H_2O_2 + CH_3O + CH_3CF_3 + 2CH_3Br \rightarrow CF_2BrCFBrOO + H_2O + 3CH_4 \quad (6)$$

$$H_2O_2 + CH_3O + CH_3CH_3 + CF_3Br + CH_3Br \rightarrow CF_2BrCFBrOO + H_2O + 3CH_4 \quad (7)$$

	B3LYP/6-311++G(d,p)		B3LYP/6-311++G(3df,3pd)		G3(MP2)B3		G3(MP2)//B3LYP 6-311++G(3df,3pd)		G4(MP2)		G4(MP2)//B3LYP 6-311++G(3df,3pd)	
isodesmic reactions	ΔH_r	$\Delta H_{f,298}$	ΔH_r	$\Delta H_{f,298}$	ΔH_r	$\Delta H_{f,298}$	ΔH_r	$\Delta H_{f,298}$	ΔH_r	$\Delta H_{f,298}$	ΔH_r	$\Delta H_{f,298}$
1	−4.8	−134.1	−5.1	−134.4	−14.4	−143.7	−14.7	−144.1	−12.2	−141.5	−9.0	−138.4
2	5.1	−134.7	4.2	−135.6	−5.6	−145.4	−6.1	−145.9	−3.6	−143.4	−0.7	−140.5
3	1.3	−134.1	1.2	−134.2	−7.9	−143.2	−8.3	−143.6	−6.0	−141.4	−6.0	−141.4
4	11.2	−134.6	10.4	−135.4	0.9	−144.9	0.4	−145.4	2.5	−143.2	2.3	−143.5
		−134.4		−134.9		−144.3		−144.7		−142.4		−140.9
5	−14.4	−117.4	−15.6	−118.6	−22.9	−125.9	−23.0	−126.0	−25.0	−128.0	−22.0	−125.0
6	−4.5	−117.7	−6.3	−119.5	−14.1	−127.6	−14.4	−127.8	−16.4	−129.9	−13.7	−127.1
7	−18.1	−117.4	−19.1	−118.4	−27.3	−126.9	−27.5	−127.1	−29.4	−129.0	−26.4	−126.0
		−117.5		−118.8		−126.8		−127.0		−128.9		−126.0

the B3LYP, G3(MP2)B3, and G4(MP2) approaches are listed in Table 4. This method requires an accurate determination of the energetics of the molecule and its constituent atoms and therefore places stringent requirements on the quantum methods employed. It is evident from Table 4 that the inclusion of d and f polarization functions in the basis set improves the angular distribution of the electron density among the bonded atoms, notably reducing the estimated B3LYP enthalpies of formation. Besides, the $\Delta H_{f,298}$ values calculated for $CF_2BrCFBrOONO_2$ and $CF_2BrCFBrOO$ at the more accurate G3(MP2)B3 and G4(MP2) levels are smaller than those calculated at the B3LYP/6-311+G(3df) level. This behavior is expected as larger electron correlation is included in the method.

As mentioned above, calculations were also performed using selected isodesmic and isogyric reaction schemes.[50] In this procedure, the enthalpy of formation for a given molecule is obtained by combining the computed isodesmic enthalpy change, ΔH_r, with well-established thermochemical data for the other molecules involved in the reaction. In these hypothetical reactions, the number of chemical bonds as well as the spin multiplicities do not change. As a consequence, systematic errors due to both incompleteness of the basis sets and deficiencies in

dx.doi.org/10.1021/jp2018617 |J. Phys. Chem. A 2011, 115, 7744–7752

Table 6. Enthalpies of Formation at 298 K[53]

species	$\Delta H_{f,298}$ (kcal mol^{-1})	species	$\Delta H_{f,298}$ (kcal mol^{-1})
H_2O	-57.798 ± 0.010	HNO_3	-32.0 ± 0.1
H_2O_2	-32.5 ± 0.05	$HOONO_2$	-12.7 ± 0.6
CH_4	-17.80 ± 0.10	CH_3Br	-9.02 ± 0.36
CH_3O	4.1 ± 0.9	CH_3CH_2Br	-14.7 ± 0.3
CH_3OH	-48.04 ± 0.14	CF_3Br	-153.3 ± 0.5
C_2H_6	-20.04 ± 0.07	CH_3CF_3	-178.2 ± 0.4

the treatment of the electron correlation energy cancel to a great extent, leading to more accurate enthalpies of formation than those obtained by atomization energies.[50,51] In this study, the working reactions listed in Table 5 were used to determine enthalpies of formation of $CF_2BrCFBrOONO_2$ and $CF_2BrCFBrOO$. The computed isodesmic enthalpy changes and derived enthalpies of formation are also included in Table 5. For these calculations we have used the reliable experimental enthalpies of formation listed in Table 6. The fact that isodesmic enthalpy changes are different from zero indicates a deviation from additivity of bond energies. However, the derived $\Delta H_{f,298}$ values are very close. On the other hand, as expected, no large basis set effects are observed. For instance, for $CF_2BrCFBrOONO_2$ only a small difference in the $\Delta H_{f,298}$ values of 0.5 kcal mol^{-1} is obtained passing from the B3LYP/6-311+G(d) to B3LYP/6-311+G(3df) method. However, the enthalpies of formation derived at the G3(MP2)B3 and G4(MP2) methods result in more negative values than obtained with the B3LYP functional, as well as with the atomization approach. In addition, good agreement between the values derived from the G3(MP2)B3 atomization energies and the isodesmic methods is apparent. This agreement is not observed for the calculations at the G4(MP2) level. To analyze the performance of the last methods, the enthalpies of formation of the four bromomethanes were estimated. The results show that both methods give good values of enthalpies of formation. However, with the G3(MP2)//B3LYP/6-311++G(3df,3pd) level the best results were obtained. For example, for CH_2Br_2 the values 0.35, 0.74, 0.83, and 1.12 kcal mol^{-1} were obtained at the G3(MP2)B3, G3(MP2)//B3LYP/6-311++G(3df,3pd), G4(MP2), and G4(MP2)//B3LYP/6-311++G(3df,3pd) levels, respectively, whereas the experimental value is 0.76 ± 0.81 kcal mol^{-1}.[52] On the other hand, it is important to note that our values agree with the experimental enthalpy of formation but differ from the recommended value in the NASA table of -2.7 ± 1.2 kcal mol^{-1}.[53] It can be seen in the list of deviations between experiment and theory for the G3/05 test set that those deviations in the G3(MP2)B3 are equal to or slightly smaller than those in G4(MP2).[30−32] Furthermore, the molecules of the G3/05 test set containing bromine are very simple, and the peroxinitrate $CF_2BrCFBrOONO_2$ is a very complex species; therefore, the deviations at the G4(MP2) for $CF_2BrCFBrOONO_2$ may increase.

For the above reasons, the best enthalpy of formation values predicted at 298 K for $CF_2BrCFBrOONO_2$ and $CF_2BrCFBrOO$ are −144.7 and −127.0 kcal mol^{-1}, derived at the G3(MP2)//B3LYP/6-311++G(3df,3pd) level of theory. The uncertainties in the employed quantum-chemical methods (close to 1 kcal mol^{-1}) and the experimental data for species in Table 6 (maximum error close to 1 kcal mol^{-1}) suggest conservative error estimates of ±2 kcal mol^{-1}.

Table 7. Calculated $CF_2BrCFBrOO-NO_2$ Bond Dissociation Enthalpy (in kcal mol^{-1}) at 298 K Derived from Isodesmic, Atomization, and Direct Methods

	ΔH_{298} (kcal mol^{-1})		
level of theory	isodesmic	atomization	direct
B3LYP/6-311+G(d)	25.1	16.8	28.4
B3LYP/6-311+G(3df)	24.3	25.3	18.6
G3(MP2)B3	25.7	25.9	26.0
G3(MP2)//B3LYP/6-311+G(3df)	26.0	25.4	25.8
G4(MP2)	21.6	21.4	20.9
G4(MP2)//B3LYP/6-311+G(3df)	23.1	21.0	20.7

Analogous to the behavior of other peroxynitrates, it is expected than the main thermal decomposition product of $CF_2BrCFBrOONO_2$ is the breaking of the $CF_2BrCFBrOO-NO_2$ bond to yield $CF_2BrCFBrOO$ and NO_2. To investigate the thermal stability of $CF_2BrCFBrOONO_2$, we estimated the dissociation enthalpy for the mentioned O−N bond. The enthalpies of formation of $CF_2BrCFBrOONO_2$ and $CF_2BrCFBrOO$ obtained from the isodesmic reaction schemes and the value of 8.17 ± 0.1 kcal mol^{-1} reported for NO_2[53] were used to calculate the bond dissociation enthalpy ΔH_{298}. This property was also calculated using the enthalpies of formation derived from atomization energies and with total energies in a direct way. The results of these three approaches are listed in Table 7. It should be noted that reliable results are obtained by using a high level of theory to estimate ΔH_{298} when calculations are performed in a direct way or from atomization energies. This result can be due to the fact that bond dissociation reactions are neither isodesmic nor isogyric. However, we used $\Delta H_{f,298}$ obtained from the isodesmic and isogyric reactions, besides of from other well-established thermodynamic data, such that this problem is largely minimized. The obtained results suggest that the G3(MP2)//B3LYP/6-311++G(3df,3pd) method improves the estimations. Our best value for the O−N bond dissociation enthalpy as derived from the best isodesmic enthalpies of formation, $\Delta H_{298} = 26.0 \pm 2$ kcal mol^{-1}, is in very good agreement with those calculated by atomization, 25.4 kcal mol^{-1}, and direct, 25.8 kcal mol^{-1}, methods. In addition, as Table 7 shows, the employment of B3LYP/6-311+G(3df) geometries in the Gaussian-3 and Gaussian-4 model chemistries does not affect appreciably the computed ΔH_{298} values.

An experimental value of $(2.2 \pm 0.5) \times 10^{-5}$ s^{-1} was obtained for the rate coefficient of $CF_2BrCFBrOONO_2 \rightarrow CF_2BrCFBrOO + NO_2$ measured at 313.4 K at pressures between 100 and 400 Torr.[24] It is very probable that the reaction was performed at the high-pressure limit. Therefore, the experimental $k_\infty = 2.2 \times 10^{-5}$ s^{-1} together with a typical Arrhenius pre-exponential factor of $A_\infty \approx 10^{15}$ s^{-1} lead to an activation energy of $E_\infty \approx 28$ kcal mol^{-1}. As usual, this value can be assimilated to ΔH_{298}. That is, the value calculated in this work of 26.0 ± 2 kcal mol^{-1} agrees satisfactorily with this one. Moreover, both are in good agreement with the average of 25 ± 1 kcal mol^{-1} proposed for species like CX_3OONO_2, where X = F, Cl.[54]

4. CONCLUSIONS

B3LYP DFT, G3(MP2)B3, and G4(MP2) model chemistry calculations have been employed to estimate several molecular

properties of the recently identified peroxynitrate $CF_2BrCFBrOONO_2$ and its radical decomposition product, $CF_2BrCFBrOO$. Equilibrium structures, harmonic vibrational frequencies, IR intensities, and assignations along with standard enthalpies of formation for the most stable conformers of $CF_2BrCFBrOONO_2$ and $CF_2BrCFBrOO$ have been determined. Enthalpy of formation values of −144.7 and −127.0 kcal mol^{-1}, respectively, were calculated from suitable isodesmic schemes for these molecules. In addition, a O−N bond dissociation enthalpy of 26.0 ± 2 kcal mol^{-1} has been estimated for $CF_2BrCFBrOONO_2$.

AUTHOR INFORMATION

Corresponding Author

*Tel.: +54-221-4257430. Fax: +54-221-4254642. E-mail: mbadenes@inifta.unlp.edu.ar.

ACKNOWLEDGMENT

This research project was supported by the Universidad Nacional de La Plata, the Consejo Nacional de Investigaciones Científicas y Técnicas (CONICET), the Comisión de Investigaciones Científicas de la Provincia de Buenos Aires (CICBA), and the Agencia Nacional de Promoción Científica y Tecnológica.

REFERENCES

(1) Stephens, E. R. *Adv. Environ. Sci. Technol.* **1969**, *1*, 119–146.
(2) Roberts, J. M. *Atmos. Environ. A* **1990**, *24*, 243–287.
(3) Nielsen, T.; Samuelsson, U.; Grennfelt, P.; Thomsen, E. L. *Nature* **1981**, *293*, 553–555.
(4) Singh, H. B. *Environ. Sci. Technol.* **1987**, *21*, 320–326.
(5) Singh, H. B.; Salas, L. J.; Viezee, W. *Nature* **1986**, *321*, 588–591.
(6) Ridley, B. A.; Shetter, J. D.; Gandrud, B. W.; Salas, L. J.; Singh, H. B.; Carroll, M. A.; Hubler, G.; Albritton, D. L.; Hastie, D. R.; Schi, H. I.; Mackay, G. I.; Karechi, D. R.; Davis, D. D.; Bradshaw, J. D.; Rodgers, M. O.; Sandholm, S. T.; Torres, A. L.; Condon, E. P.; Gregory, G. L.; Beck, S. M. *J. Geophys. Res.* **1990**, *95*, 10179–10192.
(7) Seefeld, S.; Kinnison, D. J.; Kerr, J. A. *J. Phys. Chem. A* **1997**, *101*, 55–59.
(8) Miller, C. E.; Lynton, J. I.; Keevil, D. M.; Francisco, J. S. *J. Phys. Chem. A* **1999**, *103*, 11451–11459.
(9) Tuazon, E. C.; Carter, W. P. L.; Atkinson, R. *J. Phys. Chem.* **1991**, *95*, 2434–2437.
(10) Bridier, I.; Caralp, F.; Loirat, H.; Lesclaux, R.; Veyret, B.; Becker, K. H.; Reimer, A.; Zabel, F. *J. Phys. Chem.* **1991**, *95*, 3594–3600.
(11) Sehested, J.; Christensen, L. K.; Mogelberg, T.; Nielsen, O. J.; Wallington, T. J.; Guschin, A.; Orlando, J. J.; Tyndall, G. S. *J. Phys. Chem. A* **1998**, *102*, 1779–1789.
(12) Mhin, B. J.; Chang, W. Y.; Lee, J. Y.; Kim, K. S. *J. Phys. Chem. A* **2000**, *104*, 2613–2617.
(13) Zabel, F. *Z. Phys. Chem. Bd.* **1995**, *188*, 119–142.
(14) Kirchner, F.; Mayer-Figge, A.; Zabel, F.; Becker, K. H. *J. Chem. Kinet.* **1999**, *31*, 127–144.
(15) von Ahsen, S.; Willner, H.; Francisco, J. S. *J. Chem. Phys.* **2004**, *121*, 2048–2057.
(16) Cox, R. A.; Roffey, M. J. *Environ. Sci. Technol.* **1977**, *11*, 900–906.
(17) Harwood, M. H.; Roberts, J. M.; Frost, G. J.; Ravishankara, A. R.; Burkholder, J. B. *J. Phys. Chem. A* **2003**, *107*, 1148–1154.
(18) Mazely, T. L.; Friedl, R. R.; Sander, S. P. *J. Phys. Chem. A* **1997**, *101*, 7090–7097.
(19) Mazely, T. L.; Friedl, R. R.; Sander, S. P. *J. Phys. Chem.* **1995**, *99*, 8162–8169.
(20) Libuda, H. G.; Zabel, F *Ber. Bunsen-Ges. Phys. Chem.* **1995**, *99*, 1205–1213.
(21) Varetti, E. L.; Pimentel, G. C. *Spectrochim. Acta, Part A* **1974**, *30*, 1069–1072.
(22) Tanimoto, H.; Akimoto, H. *Geophys. Res. Lett.* **2001**, *28*, 2831–2834.
(23) Grosjean, D.; Grosjean, E.; Williams, E. L. *J. Air Waste Manage. Assoc.* **1994**, *44*, 391–396.
(24) Arce, V.; dos Santos Afonso, M.; Romano, R. M.; Czarnowski, J. *J. Argent. Chem. Soc.* **2005**, *93*, 123–136.
(25) Frisch, M. J.; Trucks, G. W.; Schlegel, H. B.; Scuseria, G. E.; Robb, M. A.; Cheeseman, J. R.; Scalmani, G.; Barone, V.; Mennucci, B.; Petersson, G. A.; Nakatsuji, H.; Caricato, M.; Li, X.; Hratchian, H. P.; Izmaylov, A. F.; Bloino, J.; Zheng, G.; Sonnenberg, J. L.; Hada, M.; Ehara, M.; Toyota, K.; Fukuda, R.; Hasegawa, J.; Ishida, M.; Nakajima, T.; Honda, Y.; Kitao, O.; Nakai, H.; Vreven, T.; Montgomery, J. A., Jr.; Peralta, J. E.; Ogliaro, F.; Bearpark, M.; Heyd, J. J.; Brothers, E.; Kudin, K. N.; Staroverov, V. N.; Kobayashi, R.; Normand, J.; Raghavachari, K.; Rendell, A.; Burant, J. C.; Iyengar, S. S.; Tomasi, J.; Cossi, M.; Rega, N.; Millam, J. M.; Klene, M.; Knox, J. E.; Cross, J. B.; Bakken, V.; Adamo, C.; Jaramillo, J.; Gomperts, R.; Stratmann, R. E.; Yazyev, O.; Austin, A. J.; Cammi, R.; Pomelli, C.; Ochterski, J. W.; Martin, R. L.; Morokuma, K.; Zakrzewski, V. G.; Voth, G. A.; Salvador, P.; Dannenberg, J. J.; Dapprich, S.; Daniels, A. D.; Farkas, O.; Foresman, J. B.; Ortiz, J. V.; Cioslowski, J.; Fox, D. J. *Gaussian 09*, revision A.02; Gaussian, Inc.: Wallingford, CT, 2009.
(26) Becke, A. D. *J. Chem. Phys.* **1993**, *98*, 5648–5652.
(27) Becke, A. D. *Phys. Rev. A* **1988**, *38*, 3098–3100.
(28) Lee, C.; Yang, W.; Parr, R. G. *Phys. Rev. B* **1988**, *37*, 785–789.
(29) Frisch, M. J.; Pople, J. A.; Binkley, J. S. *J. Chem. Phys.* **1984**, *80*, 3265–3269 and references therein.
(30) Baboul, A. G.; Curtiss, L. A.; Redfern, P. C.; Raghavachari, K. *J. Chem. Phys.* **1999**, *110*, 7650–7657.
(31) Curtiss, L. A.; Redfern, P. C.; Rassolov, V.; Kedziora, G.; Pople, J. E. *J. Chem. Phys.* **2001**, *114*, 9287–9295.
(32) Curtiss, L. A.; Redfern, P. C.; Raghavachari, K. *J. Chem. Phys.* **2007**, *127*, 124105–124105−8.
(33) Badenes, M. P.; Cobos, C. J. *J. Mol. Struct. THEOCHEM* **2007**, *814*, 51–60.
(34) Badenes, M. P.; Cobos, C. J. *J. Mol. Struct. THEOCHEM* **2008**, *856*, 59–70.
(35) Troe, J *J. Chem. Phys.* **1977**, *66*, 4758–4775.
(36) Scott, A. P.; Radom, L. *J. Phys. Chem.* **1996**, *100*, 16502–16513.
(37) Haas, B.; Oberhammer, H. *J. Am. Chem. Soc.* **1984**, *106*, 6146–6149.
(38) Kopitzky, R.; Willner, H.; Mack, H. G.; Pfeiffer, A.; Oberhammer, H. *Inorg. Chem.* **1998**, *37*, 6208–6213.
(39) Marsden, C. J.; Bartell, L. S.; Diodati, F. P. *J. Mol. Struct.* **1977**, *39*, 253–262.
(40) Scheffler, D.; Schaper, I.; Willner, H.; Mack, H.-G.; Oberhammer, H. *Inorg. Chem.* **1997**, *36*, 339–344.
(41) Hermann, A.; Niemeyer, J.; Mack, H.-G.; Kopitzky, R.; Beuleke, M.; Willner, H.; Christen, D.; Schäfer, M.; Bauder, A.; Oberhammer, H. *Inorg. Chem.* **2001**, *40*, 1672–1676.
(42) von Ahsen, S.; Garcia, P.; Willner, H.; Arguello, G. A. *Inorg. Chem.* **2005**, *44*, 5713–5718.
(43) Zabel, F.; Kirchner, F.; Becker, K. H. *Int. J. Chem. Kinet.* **1994**, *26*, 827–845.
(44) Köppenkastrop, D.; Zabel, F. *Int. J. Chem. Kinet.* **1991**, *23*, 01–15.
(45) Niki, H.; Maker, P. D.; Savage, C. M.; Breitenbach, L. P. *Chem. Phys. Lett.* **1979**, *61*, 100–104.
(46) Chen, J.; Young, V.; Zhu, T.; Niki, H. *J. Phys. Chem.* **1993**, *97*, 11696–11698.
(47) Weiblen, D. G. Infrared Spectra of Fluorocarbons and Related Compounds. In *Fluorine Chemistry*; Simons, J. H., Ed.; Academic Press: New York, 1954; Vol. II.
(48) Chase, M. W., Jr. *NIST-JANAF Thermochemical Tables*, 4th ed.; *J. Phys. Chem. Ref. Data*, 1998, Monograph No. 9.
(49) Ochterski, J. W. *Thermochemistry in Gaussian*. http://www.gaussian.com/g_whitepap/thermo.htm.

(50) Hehre, W. J.; Radom, L.; Schleyer, P. v: R.; Pople, J. A. *Ab Initio Molecular Orbital Theory*; Wiley: New York, 1986.
(51) Berry, R. J.; Burgess, D. R. F., Jr.; Nyden, M. R.; Zachariah, M. R.; Schwartz, M. *J. Phys. Chem.* **1995**, *99*, 17145–17150.
(52) Lago, A. F.; Kercher, J. P.; Bödi, A.; Sztáray, B.; Miller, B.; Wurzelman, D.; Baer, T. *J. Phys. Chem. A* **2005**, *109*, 1802–1809.
(53) Sander, S. P.; Friedl, R. R.; Golden, D. M.; Kurylo, M. J.; Moortgat, G. K.; Wine, P. H.; Ravishankara, A. R.; Kolb, C. E.; Molina, M. J.; Finlayson-Pitts, B. J.; Huie, R. E.; Orkin, V. L. *Chemical Kinetics and Photochemical Data for Use in Atmospheric Studies*; NASA/JPL Data Evaluation, JPL Publication 06-2 Evaluation No. 15; NASA: Pasadena, CA, November 20, 2006. http://jpldataeval.jpl.nasa.gov/.
(54) Caralp, F.; Lesclaux, R.; Rayez, M. T.; Rayez, J. C.; Forst, W. *J. Chem. Soc., Faraday Trans. 2* **1988**, *84*, 569–585.